Original Research Paper Chemistry

Nickel Oxide and Nickel Sulphide Nanomaterials: Promising Catalysts for the Decomposition of Hazardous Dye

Sunny S. Tarve	Department of Chemistry, The Institute of Science, 15, Madam Cama Road, Mumbai-32, India.
Swapnil G. Prabhulkar	Department of Chemistry, Thakur College of Science and Commerce, Mumbai-101, India
Raju M. Patil	Department of Chemistry, The Institute of Science, 15, Madam Cama Road, Mumbai-32, India

ABSTRACT

A series of new Chiral mixed ligand (CML) ternary Nickel(II) complexes [Ni(MINAP)(aa)·2H2O] have been prepared, where MINAP is p-methylisonitrosoacetophenone as primary ligand and aa as various chiral amino acids such as L-alanine, L-valine, L-leucine, L-methionine and L-phenylalanine as secondary ligand and were characterised by various physicochemical methods. Nickel oxide (NiO) and Nickel sulphide (NiS) materials were sintered at 700°C for three hours by thermal decomposition of the CML metal complexes used as precursors. The NiO and NiS nanoparticles were characterized by X-ray diffraction (XRD), fourier transform infrared spectroscopy (FTIR) and scanning electron microscopy (SEM) with EDAX specifications. The XRD confirms single phase crystalline nature of these nanoparticles whereas the metal-oxygen and metal-sulphur bonding were confirmed by FTIR analysis. The SEM measurements obtained are indicative of formation of nano scale particles.

KEYWORDS NiO, NiS, Nanoparticles, CML-Metal complexes

INTRODUCTION

The nano sized metal powders have achieved much importance in recent times due to their wide range of applications in many fields. They possess high surface area to volume ratio due to which they exhibit physical properties which are absent in the bulk materials. Transition metal oxides such as ruthenium oxide, cobalt oxide, manganese oxide and nickel oxide are proved to be electrode materials for electrochemical capacitor[1-3]. Due to their special structures and properties nano materials are widely used in photoelectric, recording materials, catalysts, sensors, ceramic materials etc[4-7]. The nanosized nickel oxides exhibit catalytic[8,9], electronic[10,11] and magnetic[12,13] properties. One of the important applications of inorganic nanomaterials is in battery systems[14,15]. Numerous routes like thermal decomposition[16-18], carbonyl method, sol-gel technique[19], microwave pyrolysis[20], solvothermal[21], anodic arc plasma[22], sonochemical[23], precipitation-calcination[24] and microemulsion[25] have previously been investigated for production of nickel oxide nanoparticles. Most of these methods have their own advantages and limitations. The present study deals with synthesis, characterisation and applications of nickel oxide and sulphide nanoparticles by thermal decomposition of CML nickel complexes.

EXPERIMENTAL

MATERIALS

Analytical grade chemicals were used throughout with high purity. The synthesis of primary ligand i.e. sodium salt of p-methylisonitrosoacetophenone was done by using the reported method[26]. Secondary ligands L-alanine, L-valine, L-leucine, L-methionine and L-phenylalanine amino acids obtained from THOMAS BAKER and used directly without further purification. All the solvents used were distilled and purified according to standard procedures[27].

METHODS

(a) Preparation of CML Complexes:

Aqueous solutions (1mmol each) of Ni(II) sulphate heptahydrate and sodium salt of p-methylisonitrosoacetophenone were mixed slowly with constant stirring and then this mixture was kept in a boiling water bath for 30 minutes. Mixture was allowed to cool. An aqueous solution (1mmol) of the sodium salt of chiral amino acid was added to it and final mixture was refluxed for three hours in a hot water bath. Light green coloured solid complexes were obtained by filtration. Complexes were first washed with water, then with 1:1 mixture of ethanol:water and then dried over suction.

Representation of equation for formation of CML complexes can be given as follows:

$$Ni(II) + Na\text{-}MINAP + Na\text{-}aa \rightarrow (-)[Ni(MINAP)(aa)] + 2Na^{+}$$

Where Na-MINAP: Na salt of p-methylisonitrosoacetophenone, Na-aa: Na salt of L-amino acid. The complexes, formed were characterised by various physicochemical techniques[28]. The structure of the complexes predicted is as shown below.

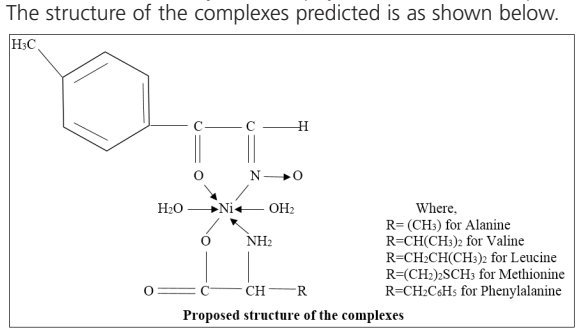

Proposed structure of the complexes

(b) Synthesis of nickel oxide and nickel sulphide nanoparticles

The chiral mixed ligand nickel complexes obtained were then subjected for heating in muffle furnace at controlled temperature of 700°C. The complexes were sintered at this temperature for three hours and then cooled to room temperature. The nickel oxide and sulphide particles thus obtained were characterised by XRD, FTIR and SEM.

The X-ray diffraction measurements of the particles were recorded on Rigaku Miniflex X-ray diffractometer using CuK→ radiation (→=1.542A°) as a source with nickel filter in the range of 20° to 80° at a scan speed of 5°/min. A Perkin-Elmer ***Precisely*** Spectrum 100 FT-IR Spectrometer was used to record FTIR spectra of all the particles in KBr between 4000-400cm^{-1} region. The SEM images were captured on Jeol Scanning Electron Microscope. The elemental analyses of the oxide and sulphide materials were done on EDAX in-built in Jeol SEM instrument.

RESULTS AND DISCUSSIONS

The powder X-ray diffraction patterns of nickel oxide and sulphide nanoparticle samples obtained from CML complexes are shown in figures1a-1e. The XRD patterns of all the nanoparticles show good crystallinity with characteristic peaks observed at 2→= 37.3°, 43.3° and 62.9° [corresponding to hkl planes of (110), (200), (220) reflection respectively][29]. The highest intensity peaks were observed between 40° and 45° for all the nanoparticles.

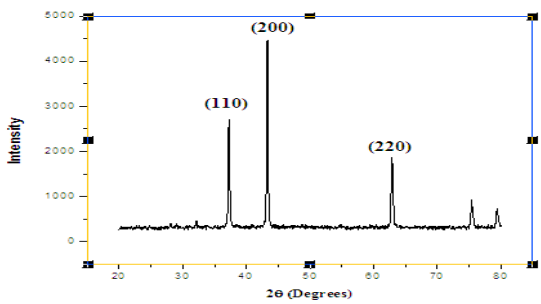

Fig.1a:XRD Pattern of Nickel Oxide Nanoparticles of [Ni(MINAP)(Ala).2H$_2$O]

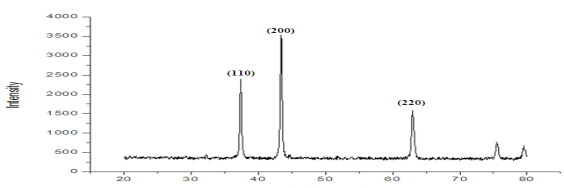

Fig.1b:XRD Pattern of Nickel Oxide Nanoparticles of [Ni(MINAP)(Val).2H$_2$O]

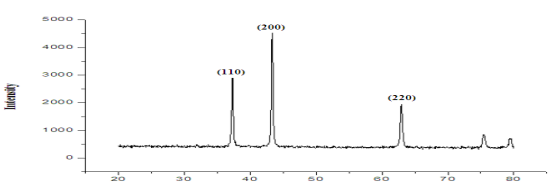

Fig.1c:XRD Pattern of Nickel Oxide Nanoparticles of [Ni(MINAP)(Leu).2H$_2$O]

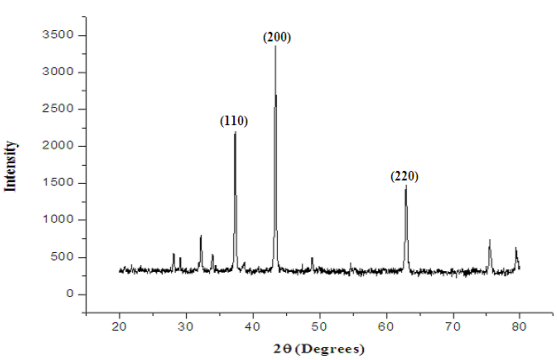

Fig.1d:XRD Pattern of Nickel Sulphide Nanoparticles of [Ni(MINAP)(Met).2H$_2$O]

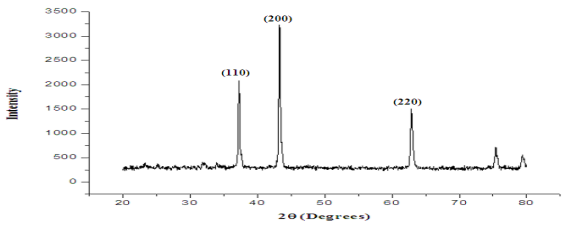

Fig.1e:XRD Pattern of Nickel Oxide Nanoparticles of [Ni(MINAP)(Phe).2H$_2$O]

All the identified peaks for NiO and NiS are assigned to the cubic phase (JCPDS file No.4-835). The diffraction peaks from X-ray diffraction data are in good agreement with the standard patterns[30,31] of NiO (JCPDS card N0. 22-1189) and NiS (JCPDS No: 89-1957). Three main diffraction peaks were indexed and found to be the face-centered cubic structure[32,33] of nanomaterials (JCPDS card No: 47-1049). There was no characteristic peak of impurity was found.

The peaks observed at about 650cm^{-1} and 480cm^{-1} in FTIR spectra of nickel oxide and sulphide particles are assigned to Ni-O and Ni-S stretching vibration mode which are the characteristic peaks for NiO and NiS nanoparticles[33-37]. The FTIR spectra of the present nickel oxide and sulphide nanoparticles prepared by CML complexes having L-Amino acids are shown in following figures 2a-2e.

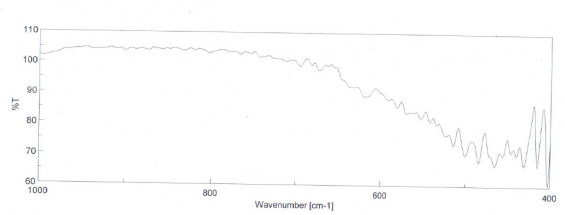

Fig.2a: FTIR Spectrum of Nickel Oxide Nanoparticles of [Ni(MINAP)(Ala).2H$_2$O]

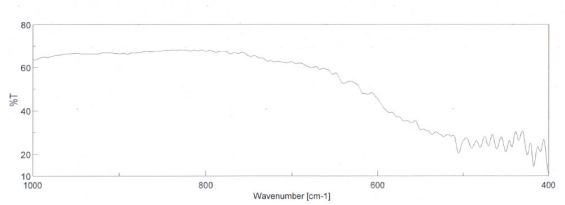

Fig.2b: FTIR Spectrum of Nickel Oxide Nanoparticles of [Ni(MINAP)(Val).2H$_2$O]

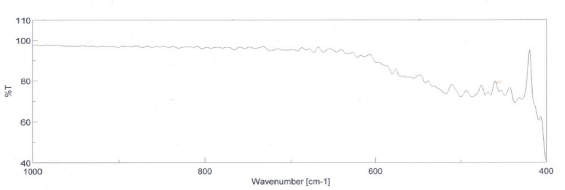

Fig.2c: FTIR Spectrum of Nickel Oxide Nanoparticles of [Ni(MINAP)(Leu).2H$_2$O]

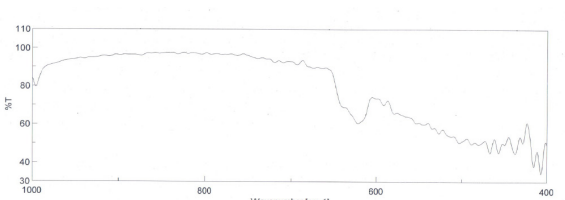

Fig.2d:FTIR Spectrum of Nickel Sulphide Nanoparticles of [Ni(MINAP)(Met).2H$_2$O]

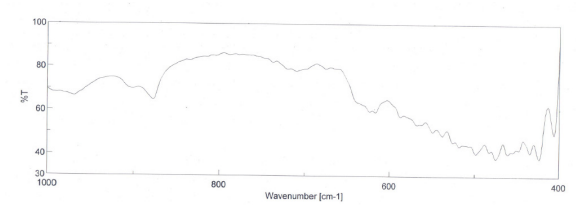

Fig.2e: FTIR Spectrum of Nickel Oxide Nanoparticles of [Ni(MINAP)(Phe).2H$_2$O]

The morphological features of the present nickel oxide and nickel sulphide nanoparticles were studied by scanning electron microscopic technique. The figures 3a-3e below depicts SEM micrograph of nanoparticles indicates the size of polycrystalline particles.

Fig.3a: SEM image of Nickel Oxide Nanoparticles of [Ni(MINAP)(Ala).2H2O]

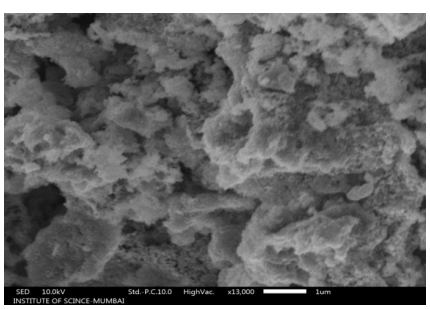

Fig.3b: SEM image of Nickel Oxide Nanoparticles of [Ni(MINAP)(Val).2H2O]

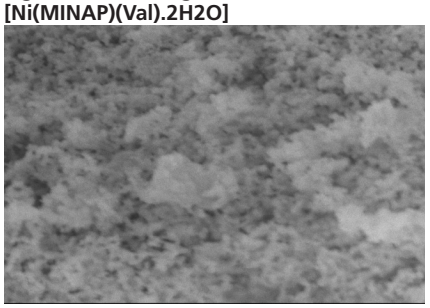

Fig.3c: SEM image of Nickel Oxide Nanoparticles of [Ni(MINAP)(Leu).2H2O]

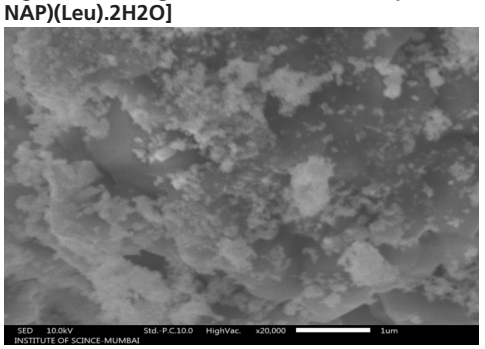

Fig.3d: SEM image of Nickel Sulphide Nanoparticles of [Ni(MINAP)(Met).2H2O]

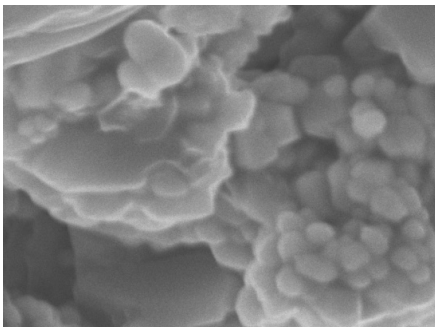

Fig.3e: SEM image of Nickel Oxide Nanoparticles of [Ni(MINAP)(Phe).2H$_2$O]

The characterisation data of all the nanoparticles is tabulated in table below.

Table 1: Analytical data of Nanoparticles

Sr. No.	Precursor Complex	Nanoparticle Obtained	FTIR		SEM
			$\bar{\nu}$ (cm^{-1})		Particle Size (nm)
1	[Ni(MINAP)(Ala).2H$_2$O]	NiO	484	654	76
2	[Ni(MINAP)(Val)·2H$_2$O]	NiO	480	652	61
3	[Ni(MINAP)(Leu)·2H$_2$O]	NiO	486	650	74
4	[Ni(MINAP)(Met)·2H$_2$O]	NiS	480	649	63
5	[Ni(MINAP)(Phe)·2H$_2$O]	NiO	481	655	79

APPLICATIONS

Azo dyes are the most commonly used synthetic dyes in many industries, laboratories etc. which are usually major pollutants of natural water resources. Due to their loss in drainage system with intensive colour and toxicity they are highly hazardous and even mutagenic at low concentrations to animal and plant kingdom in the ecosystem. Hence, it becomes necessary to degrade these dyes and control their activity by altering their toxic effects towards lower toxicity before disposing them as effluents into sewage.

The present nanomaterials were applied for the photocatalytic degradation of potentially hazardous Thiazole Yellow G (TYG) dye in a homemade photo-reactor by NiO and NiS nanoparticles obtained from [Ni(MINAP)(Val).2H$_2$O] and various parameters such as contact time, amount of nanomaterial, type of nanomaterial were optimized for aliquot of the dye solution at λmax of TYG at 405nm. The nanomaterials in the present study were found to be effective for TYG degradation under optimized reaction conditions and the remnant concentration of the dye 'X(%)' and percentage degradation %D values are tabulated for various parameters as below.

Effect of time:

The time required for the degradation of the TYG (100 ppm) was studied from 0 to 240 minutes. It was found that, the time required for optimum percentage of degradation (%D) of the dye was three hours. The observations obtained are tabulated in the table below.

Table 2: Effect of Time on TYG degradation

Time (min)	Absorbance (A_o)	X (%)	% D
00	0.742	100.000	0.000
15	0.742	100.000	0.000
30	0.742	100.000	0.000
45	0.742	100.000	0.000
60	0.693	93.396	6.604

75	0.673	90.701	9.299
90	0.604	81.402	18.598
105	0.535	72.102	27.898
120	0.466	62.803	37.197
135	0.397	53.504	46.496
150	0.328	44.205	55.795
165	0.259	34.906	65.094
180	0.190	25.606	74.394
195	0.122	16.442	83.558
210	0.052	7.008	92.992
225	0.052	7.008	92.992
240	0.052	7.008	92.992

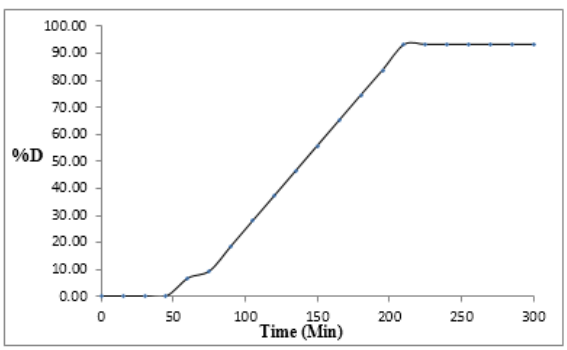

Fig.4 :Time Vs %D

Effect of amount of catalyst:
The different concentrations of catalyst were studied to get maximum degradation of TYG dye at optimum time interval. The resultant findings are shown in the following table 3.

Table 3: Effect of Amount of Catalyst on TYG degradation

Amount of catalyst (g)	Absorbance (A_0)	X(%)	%D
0.025	0.111	14.960	85.040
0.050	0.052	7.008	92.992
0.075	0.052	7.008	92.992
0.100	0.052	7.008	92.992
0.125	0.052	7.008	92.992
0.150	0.052	7.008	92.992
0.175	0.052	7.008	92.992
0.200	0.052	7.008	92.992
0.225	0.052	7.008	92.992
0.250	0.052	7.008	92.992

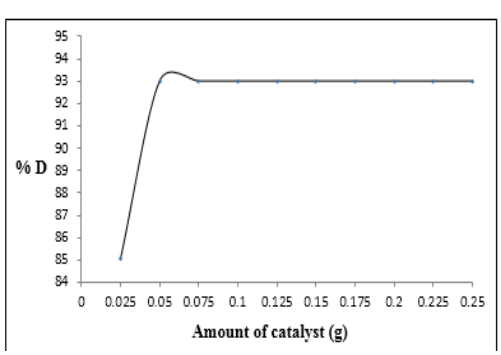

Fig.5: Amount of Catalyst Vs %D

Percentage Degradation of TYG over various Nickel nanoparticles
Following table shows the percentage degradation of TYG dye by using present nano materials at optimum concentration in optimised time.

Table 4: Percentage Degradation of TYG over present NiO/ NiS nano materials

Sr. No.	Precursor Complex	Nano-material formed	Absorb-ance (A_0)	X (%)	%D
1	[Ni(MINAP) (Ala).$2H_2O$]	NiO	0.163	21.968	78.032
2	[Ni(MINAP) (Val)·$2H_2O$]	NiO	0.051	6.873	93.127
3	[Ni(MINAP) (Leu)·$2H_2O$]	NiO	0.157	21.159	78.841
4	[Ni(MINAP) (Met)·$2H_2O$]	NiS	0.055	7.412	92.588
5	[Ni(MINAP) (Phe)·$2H_2O$]	NiO	0.178	23.989	76.011

Reusability of the catalyst:
The spent nano materials were removed by centrifugation from decomposed dye solution and were washed with double distilled hot water followed by acetone; again centrifuged and dried in an air drying oven. After cooling to room temperature the recovered catalyst particles were used effectively at least for five cycles for the decomposition of TYG dye over a period of times. The possible phase changes, if any, were checked by scanning of fresh and spent catalyst in Rigaku Miniflex X-ray diffractometer, which shown no serious phase alterations.

Table 5: Reusability of the catalyst

No, of Catalytic Cycles	Absorbance (A_0)	X (%)	%D
1	0.051	6.873	93.127
2	0.051	6.873	93.127
3	0.051	6.873	93.127
4	0.052	7.008	92.992
5	0.052	7.008	92.992
6	0.054	7.278	92.722

REACTION MECHANISM OF DECOMPOSITION OF TYG DYE:
The probable mechanism of decomposition of TYG dye using present nanomaterials as catalyst may be represented as follows.

$$^1TYG_0 \xrightarrow{h\nu} {}^1TYG_1$$

$$^1TYG_1 \xrightarrow{ISC} {}^3TYG_1$$

$$NiO\text{-}P/NiS\text{-}P \xrightarrow{h\nu} e^-(CB) + h^+(VB)$$

$$^3TYG_1 + h^+ \xrightarrow{h\nu} \text{Leuco } TYG^+$$

$$\text{Leuco } TYG^+ \xrightarrow{h\nu} \text{Colourless solution}$$

The radiations in the visible region of EMR are absorbed by Thiazole Yellow G ($^1TYG_0$) and generate its excited singlet state ($^1TYG_1$). This excited singlet state undergoes intersystem crossing (ISC) and gives the triplet state ($^3TYG_1$) of TYG. The NiO and NiS nanoparticles absorb the light energy to excite its electron (e^-) from valence band (VB) to the conduction band (CB) of nanoparticles (NiO-P/NiS-P) and a hole (h^+) is created in

valence band. The holes in the valence band of semiconducting nanoparticles oxidize the dye molecules to its leuco form (TYG^{+}) and as a consequence, decomposition of the dye results to the bleaching of TYG dye.

CONCLUSION

The nickel oxide and nickel sulphide nanoparticles synthesized, characterized and were successfully applied to the photocatalytic degradation of environmentally hazardous Thiazole Yellow G dye in the present study. The optimum conditions were set by various parameters such as equilibration time, catalyst selection, catalyst concentration and it was found that the NiO and NiS nanoparticles in the present study gave optimum degradation of TYG dye in three hours with 0.050 grams of the photocatalyst NiO nanoparticles obtained from [Ni(MINAP)(Val).$2H_2O$] were found more effective.

REFERENCES

1. P. Simon, Y. Gogotsi; Nat. Mater., 7, 845, 2008.
2. D. Pan, S. Ma, X. Bo and L. Guo; Microchim. Acta., 173, 215, 2011.
3. N. A. Yusof, N. Daud, S. Z. M. Saat, T. W. Tee and A. H. Abdullah; Int. J. Electrochem. Sci., 7, 10358, 2012.
4. Y.S. Kim, Y.H. Kim; J. Magn. Magn. Mater., 267, 105, 2003.
5. J.J. Shi, Y.F. Zhu, X.R. Zhang, R.G.B. Willy, R.G.C. Ana; Trac- Trends Anal. Chem., 23, 351, 2004.
6. D.Y. Goswami, S. Vijayaraghavan, S. Lu, G. Tamm; Sol. Energ., 76, 33, 2004.
7. M. Conte, P.P. Prosini, S.Passerini; Mater. Sci. Eng., B 108, 2, 2004.
8. K.M. Dooley, S.Y. Chen, J.R.H. Ross; J. Catal., 145, 402, 1994.
9. A. Alejandre, F. Medina, P. Salagre, A. Fabregat, J.E. Sueiras; Appl Catal., B 18, 307, 1998.
10. L. Soriano, M. Abbate, J. Vogel, J.C.Fuggle; Chem. Phys. Lett., 208, 460, 1993.
11. V. Biji, M.A. Khadar; Mater. Sci. Eng., A 304, 814, 2001.
12. R.H. Kodama, S.A. Makhlouf, A.Berkowitz; Phys. Rev. Lett., 79, 393, 1997.
13. R.H. Kodama; J. Magn. Magn. Mater., 200, 359, 1999.
14. F. Li, H. Chen, C. Wang, K. Hu; J. Electroanal. Chem., 531, 53, 2002.
15. Y. Nuli, S. Zhao, Q. Qin; J. Power Sources, 114, 113, 2003.
16. W. Wang, Y. Liu, C. Xu, C. Zheng, G. Wang; Chem Phys Lett., 362, 119, 2002.
17. N.M. Hosny; Polyhedron, 30, 470, 2011.
18. X. Li, X. Zhang, Z. Li, Y. Qian; Solid State Commun, 137, 581, 2006.
19. L. Xiang, X.Y. Deng, Y. Jin; Scr. Mater., 47, 219, 2002.
20. Y. Wang, J. J. Ke; Mater. Res. Bull., 31, 55, 1996.
21. K. Anandan, V. Rajendran; Solid State Electron, 14, 43, 2011.
22. Z. Wei, H. Qiao, H. Yang, C. Zhang, X. Yan; J. Alloys Compd., 479, 855, 2009.
23. S. Mohseni Meybodi, S.A. Hosseini, M. Rezaee, S.K. Sadrnezhaad, D. Mohammadyani; Ultrason Sonochem, 19, 841, 2012.
24. X. Deng, Z. Chen, Mater Lett, 58, 276, 2004.
25. Y. Du, W. Wang, X. Li, J. Zhao, J. Ma, Y. Liu, G. Lu; Mater Lett, 68, 168, 2012.
26. F. J. Welcher; Organic Analytical Reagents. Vol. III De Van Nostrand N.Y, 1955.
27. B. S. Furnis, A. J. Hannaford, P. W. G. Smith and A. R. Tatchell; Vogel's Textbook of Practical Organic Chemistry 5th Ed. ELBS Longman London, 1989.
28. Sunny S. Tarve, Sagar V. Sanap, Raju M. Patil; Indian Journal of Applied Research; 5(4), 17, 2015.
29. Kai Wang, Liwei Li and Hongwei Zhang; Int. J. Electrochem. Sci., 8, 8785, 2013.
30. D. Mohammadyani; 2nd International Conference on Ultrafine Grained & Nanostructured Materials (UFGNSM), International Journal of Modern Physics: Conference Series, Vol. 5, 270, 2012.
31. H. Gleiter; Prog. Mater. Sci., 33, 223, 1989.
32. Yu Luo, Jiancheng Zhang, Yue Shen, Shutao Jianf and Guoyong Liu; J. Mater. Sci. Technol., 23(5), 587, 2007.
33. Rajesh Kumar, Ashwani Sharma, Nawal Kishore, Narender Budhiraja; International Journal of Engineering, Applied and Management Sciences Paradigms, 6(1), 64, 2013.
34. S. G.Prabhulkar and R. M. Patil; Research Journal of Material Sciences (International Science Congress Association), 1(4), 2013.
35. S. G. Prabhulkar and R. M. Patil; Research Journal of Material Sciences (International Science Congress Association), 1(9), 1, 2013.
36. P. Ouraipryvan, T. Sreethawong, S. Chavadej; Mater. Lett., 63, 1862, 2009.
37. M. Kanthimathi, A. Dhathathreyan and B. V. Nair; Mater. Lett., 58, 2914 , 2004.